Published in final edited form as:

J Neurochem. 2021 March ; 156(6): 819–833. doi:10.1111/jnc.15137.

Ganglioside GD3 regulates dendritic growth in newborn neurons in adult mouse hippocampus via modulation of mitochondrial dynamics

Fu-Lei Tang, **Jing Wang**, **Yutaka Itokazu**, **Robert K. Yu***

Department of Neuroscience and Regenerative Medicine, Medical College of Georgia, Augusta University, Augusta, Georgia 30912, U. S. A.

Abstract

Ganglioside GD3, a major ganglioside species in neural stem cells, plays a crucial role in maintenance of the self-renewal capacity of these cells. However, its bioactivity in postnatally differentiated neurons in the neurogenic regions of adult brains has not been elucidated. Here, we describe for the first time that deletion of GD3 not only impairs neurotrophin-induced stem cell proliferation, but also alters the dendritic structure as well as the number of synapses of nascent neurons in the dentate gyrus (DG) of adult brain. When examining the behavioral phenotypes, GD3-KO mice displayed impairment in hippocampus-dependent memory function. To further gain insight into its cellular function, we examined GD3-binding partners from mouse brain extract using a GD3-specific monoclonal antibody, R24, followed by LC-MS/MS analysis and identified a mitochondrial fission protein, the dynamin related protein-1 (Drp1), as a novel GD3-binding protein. Biochemical and imaging analyses revealed mitochondrial fragmentation in GD3-depleted DG neurons, suggesting that GD3 is essential for the mitochondrial Drp1 turnover that is required for efficient mitochondrial fission. These results suggest that GD3 is required for proper dendritic and spine maturation of newborn neurons in adult brain through the regulation of mitochondrial dynamics.

Keywords

Ganglioside GD3; adult neurogenesis; neuronal morphogenesis; dynamin-related protein-1; mitochondrial dynamics

Introduction

Gangliosides are a class of important sialic acid-containing glycosphingolipids (GSLs) that are most abundant in brain tissues and widely distributed on the outer surface of nerve

***Corresponding author** Dr. Robert K. Yu, Department of Neuroscience and Regenerative Medicine, Medical College of Georgia, Augusta University, 1120 15th St., Rm. CA1006, Augusta, GA 30912, U. S. A., Telephone: 706-721-8931; ryu@augusta.edu.

Authors' contributions

F.T. and R.K.Y. conceived and designed the project, and wrote the manuscript. F.T. and J.W. performed all the experiments and analyses. J.W., Y.I. and R.K.Y. helped with data interpretation and provided instructions. R.K.Y. supervised the project. All authors read and approved the final manuscript.

Competing interests: The authors declare that they have no competing interests.

cells. It is generally accepted that they play a critical role in neural development (Yu et al. 2012). The expression of gangliosides during brain development is cell-specific and developmentally regulated; it shifts from an abundance of simple gangliosides, such as GM3 and GD3, to a group of complex gangliosides, such as GM1, GD1a, GD1b, and GT1b (Yu & Ando 1980; Yu et al. 2011; Schnaar et al. 2014). Ganglioside GD3 is first expressed in the neural tube during early development and can be detected using a GD3-specific monoclonal antibody (mAb R24) (Rosner et al. 1992). In cultured mouse neural stem/progenitor cells (NSCs/NPCs), GD3 is the predominant ganglioside species, accounting for more than 80% of the total gangliosides (Yanagisawa et al. 2005). [Footnote: The cells we isolated from mouse brain consist largely of a mixture of NSCs and NPCs that share many common properties, such as high proliferative potential, the capacity for self-renewal and multipotency. As development proceeds, NSCs become less abundant and the more restricted NPCs emerge. For simplicity, we denote the cell population used in this investigation as NSCs.] In adult mouse brain, GD3 is abundant in the dentate gyrus (DG) of hippocampus, one of the main brain regions continuously generates new neurons during adulthood (Wang et al. 2014). By studying GD3-synthase knockout (GD3S-KO) mice, we found that ablation of GD3 in NSCs coincides with its inability to facilitate EGF-induced cell proliferation and maintain NSC pools (Wang & Yu 2013; Wang et al. 2014), but little is known on the role of GD3 in modulating dendrite branching and synaptic plasticity in these nascent granule cells (GCs) in adult hippocampus. For this reason, we initiated a detailed study to investigate the role of GD3 in determining the relationship between the cellular morphology of the newly formed GCs in DG and its relationship with hippocampus-dependent memory using loss-of-function approaches in adult mice.

Neurons differentiated from NPCs undergo morphological changes which required a huge amount of energy (Son & Han 2018). The mitochondria is the main intracellular organelle for producing adenosine triphosphate (ATP) (Chandel 2014). It is thus not surprising to find that mitochondria play a crucial role in adult neurogenesis (Beckervordersandforth et al. 2017; Son & Han 2018). GD3 has been found in the mitochondrial membrane using immunoelectron and confocal microscopy (De Maria et al. 1997; Rippo et al. 2000; Garcia-Ruiz et al. 2002); presumably it plays a specific role in regulating neuronal morphology/function of those nascent neurons.

In the present study, we found that GD3 was expressed in NSCs and immature neurons in the DG. Using a GD3S-KO mouse model, we demonstrated that GD3 was required in the morphological differentiation *in vivo*. Furthermore, GD3-depleted mice displayed impairment in the novel object recognition (NOR) task and the Barnes maze test, which indicated that GD3 played a role in hippocampus-dependent memory. To gain further insight into its cellular function, we examined GD3-binding partners by LC-MS/MS analysis and identified mitochondrial fission protein dynamin-related protein 1 (Drp1) as a new GD3-binding protein. The physiological significance of the GD3-Drp1 interaction may be related to Drp1 turnover in the mitochondria that is necessary for efficient mitochondrial fission. These findings clearly implicate GD3 as playing a crucial role in hippocampus-dependent functions by controlling dendritic arborization through modulation of mitochondrial dynamics.

Materials and Methods

Animals

The experiment details are described in a flow sheet shown in Figure 1. Mice were maintained and cared for according to animal protocols approved by the Institute of Animal Care and Use Committee (IACUC) at Augusta University (AU) (Ref: AUP 2009-0240). GD3S-KO mice (RRID:MMRRC_000037-MU) were kindly provided by Dr. Richard Proia (National Institutes of Health, Bethesda, MD, USA.) and cared as described previously (Wang et al. 2014). The following primers were used for genotyping: GD3S 9692: 5'-CAC AGT TAC ATC TAC ATG CCT-3'; GD3S 9694: 5'-GCA AGA CGT TGT CAT AGT AGT-3'; and RLP290 (Neo): 5'-TCG CCT TCT TGA CGA GTT CTT CTG AG-3'. All phenotypic characterizations were performed in GD3S-KO and their control mice in a C57BL/6 background. Both male and female mice were used in all experiments except for behavior tests when only male mice were used. The study was not pre-registered and was exploratory. No animals were excluded in this study.

Retrovirus stereotactic injections

Retrovirus were prepared as described by previously described procedures with minor modifications (Steib et al. 2014; Sun et al. 2018; Schaffner et al. 2018). Briefly, plasmids were transfected into cultured 293-GPG cells (RRID:CVCL_E072) using polyethyleneimine, and retroviral particles containing supernatant were collected at 48 hours and 72 hours post transfection, filtered by a 0.44-μm filter, and then concentrated at 28,000 rpm for 2 hours. For injections, two-month-old mice (n=30) were deeply anesthetized with 2% isoflurane (Piramal Healthcare) through a vaporizer (Kent Scientific). Mice were stereotactically injected with 1 μl of the retroviruses into the left and right DG (−1.9 mm anterior/posterior, ±1.6 mm medial/lateral, −1.9 mm dorsal/ventral from dura) at a rate of 0.5 μl/min. After the surgery, we injected the mice subcutaneously with the analgesic buprenorphine (0.1 mg/kg) to relieve pain.

Tissue processing and immunofluorescent staining procedures

Mice were first transcardially perfused with 30 ml phosphate-buffered saline (PBS, pH 7.4) and followed by 50 ml of 4% paraformaldehyde (PFA). The brains were removed and fixed in 4% PFA for another 4 hours at room temperature. Coronal sections were prepared by a vibratome (VT1000s, Leica) and the tissue sections were analyzed by immunostaining.

Immunofluorescent staining of floating sections was performed as described previously (Tang et al. 2015). The primary antibodies were: rabbit anti-GFP (1:500; Invitrogen, RRID:AB_221569), mouse anti-nestin (1:200; Millipore, RRID:AB_94911), goat anti-DCX (1:500; Santa Cruz, RRID:AB_2088494), and rabbit anti-Drp1 (1:500, Cell Signaling, RRID:AB_10950498).

Mouse anti-GD3 monoclonal antibody, clone R24 (kindly provided by Dr. Lloyd J. Old at the Memorial Sloan-Kettering Cancer Center, New York, NY), generated as described originally (Pukel et al. 1982). Any custom-made material reported in this investigation will be shared upon reasonable request.

Confocal images were taken by Nikon A1 confocal as describe previously (Tang et al. 2020). Sections for dendritic morphology analysis were 100-μm thick, and sections for spine morphology analysis were 35-μm thick. In addition, a 3x zoom was used for spine analysis. 3D reconstructions were performed by using the Filament Tracer and Surface Tracer tools in Imaris.

Behavioral analysis—Two-month-old male mice were used for behavioral studies as described previously (Lu et al. 2019).

Open-field test—The mouse was placed at one corner of a 56 cm × 56 cm arena at the beginning, making it face the wall. The number of episodes of rearing and grooming, travel distance, and the time spent in a delineated center zone (26 cm × 26 cm) were recorded during a 5-min free-moving period.

Novel object recognition (NOR) test—Each mouse was placed in a 56 × 56 cm arena, with two identical objects placed at each end of the arena. After 10 min of investigation, mice were returned to their home cage. 24 hours later, one test object was replaced with a novel object (the same height and volume, but had a different shape and appearance as the familiar object), and animals were allowed 5 min for investigation. The time spent exploring each object was recorded.

Barnes maze task—At trial stage (days 1 to 3), a video camera controlled by ANY-maze video-tracking software was used to record the escape latency of the mouse from the center of platform to the hidden chamber, its escape velocity, and its escape traces. On the probe day (day 4), the hidden chamber was removed. The escape latency and quadrant occupancy were recorded.

Immunoprecipitation of GD3 interacting proteins

Three embryonic day 14.5 (E14.5) mouse brains were homogenized in 10 ml of a homogenization buffer (250 mM sucrose, 20 mM Tris·HCl, pH 7.8) with protease inhibitors as described previously (Savas et al. 2015). The homogenate was centrifuged at 1,500 x g for 15 min and the pellets were resuspended by gently pipetting up and down in a total volume of 4 ml of homogenate buffer and then lysed by passing through a 22-G needle 20 times. After centrifugation at 1,000 × g for 10 min, the supernatants were collected for the bind assay. 100 ul G Dynabeads were first incubated with 2 ug of mAb R24 antibody or IgG for 1 hour at room temperature, then added to an equivalent amount of brain extract. The mixture was kept overnight at 4°C with rotation.

Beads bound with proteins were magnetically captured and washed 3 times with PBS. Samples were separated on 4-12% precast gels and subjected to LC–MS/MS analysis on an Orbitrap Velos (Thermo) mass spectrometer as previously described (Savas et al. 2015).

Glycosphingolipid-coated bead assay

His-tagged human Drp1 was purified from the cell lysate of HEK293T cells transfected with a His-Drp1 construct using cobalt beads. The GSL-coated bead assay was performed

following a previous report (Yoon et al. 2006). Briefly, Gangliosides GD3, GM3 and GM1 (24 ug each) were dried and re-dissolved in an ethanol/water solution (9:1) and were incubated with the polystyrene beads (1-μm in diameter; Sigma-Aldrich) 1 hour at room temperature. After washing with PBS, the GSL-coated beads were resuspended in a His-Drp1 solution. The mixture was kept overnight at 4°C with rotation and then washed three times with PBS. Proteins bound to GSL-coated beads were denatured with SDS sample buffer at 90°C and analyzed by Western blotting with the anti-Drp1 antibody.

Isolation of mitochondria

Percoll density gradient centrifugation was used to isolate the mitochondria. Tissues in the DG region were dissected out as described previously (Hagihara et al. 2009) and homogenized in isolation buffer (225 mM mannitol, 75 mM sucrose, 1 mM EGTA, 5 mM HEPES, pH = 7.2). After centrifugation at 1,100 g for 2 min, the supernatant was mixed with 80% Percoll and carefully layered on the top of 10% Percoll, then centrifuged at 18,500 g for 10 min. The myelin-rich top fraction was removed, leaving the mitochondrion-enriched pellet at the bottom. The isolated mitochondria were washed once and then lysed with SDS sample buffer.

A sample containing 10 to 20 μg of total protein was loaded onto 8% or 14% sodium dodecylsulfate (SDS) gels. Following electrophoresis, gels were transferred onto Nitrocellulose Blotting Membranes (Bio-Rad). Antigen-specific primary antibodies, including rabbit anti-Drp1 (1:200; Cell Signaling, RRID:AB_11178938), rabbit anti-phospho-Drp1 (1:1000, Cell Signaling, RRID:AB_11178659), mouse anti-Mfn2 (1:2000; Abcam, RRID:AB_2142629), mouse anti-beta-Catenin (1:2000; Abcam, RRID:AB_562065), rabbit anti-Vps35 (1:200; Abcam, RRID:AB_1524565), mouse anti-VCP (1:2000; Millipore, RRID:AB_10806328), mouse anti-Atp1a1 (1:1000; Santa Cruz, RRID:AB_1125502), mouse anti-tubulin (1:8000; Proteintech, RRID:AB_2687491), and rabbit anti-VDAC (1:5000, Abcam, RRID:AB_297264).

NSC isolation and differentiation analysis

NSCs were isolated and prepared as described previously (Wang & Yu 2013). Briefly, tissues in the DG regions were dissected and treated with papain and then mechanically dissociated in HBSS to obtain single-cell suspensions. Cells were seeded at a density of 5,000–10,000 cells/ml and cultured in a medium containing Neural Basal Medium (2% B27, 1x GlutaMAX, 2 μg/ml heparin, 50 units/ml penicillin/streptomycin, 20 ng/ml epidermal growth factor (EGF), and 20 ng/ml fibroblast growth factor (FGF) for 7 days.

The neurospheres were dissociated with Accutase into single cells and seeded to a density of 100,000 cells per well on poly-*D*-lysine (PDL)/laminin-coated glass coverslips. After 24 hours, the growth medium was replaced by the growth medium without EGF and FGF. After another 24 hours, cells were transduced with a CAG-Mito-dsRed retrovirus for labeling mitochondria.

Differentiated cells were fixed for 10 min in 4% PFA and permeabilized with 0.1% saponin for 15 min. Cells were incubated for 1 hour with primary antibodies, mouse anti-GD3

antibody (1:500) and rabbit anti-Drp1 (1:200), rinsed with PBS-0.0025% saponin and incubated for 45 min with secondary antibodies.

Mitochondrial morphology analysis

Mitochondrial morphology was quantified as previously described (Tang et al. 2015; Wang et al. 2016). Raw images were background-corrected, linearly contrast-optimized to generate binary images. Most mitochondria were well separated in binary images and large clusters of mitochondria were excluded automatically. All binary images were analyzed by ImageJ software to provide information about the mitochondrial aspect ratio (the ratio between major and minor axes of an ellipse equivalent to the mitochondrion as an index for mitochondrial morphology).

Statistics

Blinding was achieved in all experiments since experimenters were always unaware of the animal's genotyping during *in vitro* or behavioral experimentation and while performing all different analyses. There was no test for outliers and no pre-determined exclusion criteria. Although no statistical methods were used to pre-determine sample size, our sample sizes were determined as described previously (Tang et al. 2015; Wang et al. 2014). GraphPad Prism 8 (GraphPad Software, RRID:SCR_002798) was used for statistical analysis. All data sets were analyzed using D'Agostino–Pearson omnibus test and Shapiro–Wilk test for normality. Data sets with normal distributions were analyzed for significance using either unpaired Student's two-tailed *t*-test or one-way ANOVA test. When data were not normally distributed the Mann-Whitney U test was used. The significance levels were expressed as $*p < 0.05$, $**p < 0.01$, $***p < 0.001$, and all data presented as mean ± s.e.m.

Results

GD3 is expressed in NSCs and immature neurons in the DG of adult hippocampus

To investigate the function of GD3 in adult hippocampus, we first analyzed the expression of GD3 in the DG of 2-month-old mice by immunofluorescence microscopy. As shown in Fig. 2A, GD3 is abundantly expressed in the subgranular zone (SGZ) of the DG where NSCs reside. In agreement, GD3 staining was detected in cells expressing the radial glia-like NSC marker, Nestin. In GD3S-KO mice, where GD3 was not expressed, the GD3 staining signal was absent (Fig. 2B-C), demonstrating the specificity of the anti-GD3 monoclonal antibody, mAb R24. Also, GD3 partially colocalized with doublecortin (DCX, an immature neuronal marker) positive cells) (Fig. 2B-C). GD3 staining was observed in both cell bodies and dendrites of DCX-positive cells present in the granule cell layer (GCL). These results are consistent with the notion that GD3 is expressed in NSCs and immature neurons in the SGZ (Fig. 2C). This expression pattern suggests that GD3 not only plays a critical role in the regulation of NSC proliferation during early stages of brain development (Wang and Yu, 2013), but also functions during later stages of neurogenesis.

GD3 is necessary for the dendritic maturation of nascent granule neurons

Previously, we have shown a progressive loss of the NSC pool in the DG of GD3S-KO mice, suggesting that GD3 may also play a crucial role in the long-term maintenance of

NSC populations in postnatal mouse brain (Wang et al. 2014). We next investigated whether integration of these nascent granule neurons into the existing circuitry would be impaired in the absence of GD3. The CAG-GFP retrovirus was stereotactically injected into the DG of 2-month-old GD3S-KO and WT mice. Animals were sacrificed at 14, 28, and 42 days post-retrovirus injection (dpi), (Fig. 3A). In contrast to previous findings (Wang et al. 2014), we found fewer GFP-labeled nascent neurons in GD3S-KO mice, suggesting that GD3S-KO could suppress the activation of NSCs.

Since the integration of nascent neurons into the existing cytoarchitecture is expected to involve progression through a series of morphological stages of maturation, we focused on dendritic arborization and synapse formation. We performed confocal microscopic analysis followed by 3D reconstruction and morphometric evaluation of the dendritic arbor in labeled neurons and found that the total number of dendritic branches and their lengths were significantly reduced in GD3S-KO vs. control neurons at 28 and 42 dpi (Fig. 3B-D). Moreover, Sholl analysis (Bird & Cuntz 2019) revealed that the dendritic complexity of GD3S-KO neurons was reduced compared with control neurons at 42 dpi (Fig. 3F).

We next analyzed the impact of GD3S-KO on dendritic spine formation. High-magnification imaging analysis of dendritic spines showed reduced spine density of GD3S-KO neurons compared to their respective controls at all time points (Fig. 3G-H). 3D-analysis of spine morphology showed that GD3S-KO neurons had fewer mushroom spines than those in the WT controls, suggesting compromised dendritic spine formation. These data showed that GD3 is involved in the control of dendrite and spine development and may affect the integration of newborn DG neurons in adult brain into the hippocampal circuitry.

Hippocampus-dependent memory is impaired in GD3S-KO mice

To test whether GD3 plays a role in hippocampus-dependent memory, we subjected 2-month-old GD3S-KO male mice and their WT littermates to three behavioral tests. First, the open-field test was used to examine the locomotor activity (Fig. 4A). We found that GD3S-KO mice exhibited similar rearing times (data not shown) and travel distance (Fig. 4B) compared with the control littermates, suggesting that locomotor functions were not affected. Likewise, we also found that the grooming time (data not shown) and time spent in the central zone (Fig. 4C) for GD3S-KO mice were indistinguishable from controls, suggesting that GD3S-KO mice did not exhibit abnormal anxiety levels. Next, we subjected these mice to the novel object recognition (NOR) task, a hippocampus-dependent memory test (Ennaceur & Delacour 1988). During the training session (two identical objects), no preference was detected for one object over the other in both genotypes (Fig. 4D-E); however, during the test session, whereas WT mice presented a preferential exploration toward the novel object, GD3S-KO mice exhibited a significant decrease in preference to explore the novel object (Fig. 4D-E).

The impairment in hippocampal-dependent memory shown by GD3S-KO mice was corroborated using the Barnes maze task. This task requires the animal to encode spatial information into a memory and use that memory to complete an escape task (Harrison et al. 2009). The results revealed that GD3S-KO mice displayed a significant spatial memory defect as evidenced by an increase in escape latency to find the hidden chamber on the third

day of the training trial, with decreased quadrant occupancy on the probe trial compared with the control mice (Fig. 4F-H). The escape velocity was similar between the two groups, indicating that differences in escape latencies were not due to speed variations. These results indicate impairment of the spatial memory in GD3S-KO mice and support that GD3 is required for a proper function of hippocampus-dependent memory.

Identification of Drp1 as a GD3-binding protein

Gangliosides regulate cell signaling often by associating with proteins (Schnaar 2016). To better understand how GD3 regulates adult hippocampal neurogenesis, we performed a mass spectrometric (MS) analysis-based proteomic screen for GD3-protein interactors. We first performed affinity chromatography using the anti-GD3 mAb R24 and detergent-free brain extract, followed by MS analysis (Fig. 5A). Coomassie staining showed an enrichment of proteins in the anti-GD3 pulldown lanes, which was absent when the anti-GD3 antibody was omitted or using the GD3S-KO brain extract as the prey. In addition to EGFR, which has been shown to bind with GD3 in NSCs to maintain the self-renewal capability of NSCs (Wang & Yu 2013), we identified several other proteins from the screening (Fig. 5B, C). Previously, we showed that GD3 mediated EGFR intracellular trafficking/degradation and that decreased EGFR expression was found in the GD3S-KO NSCs (Wang & Yu 2013). In the present study, we tested the impact of GD3 deficiency on expression of these new binding proteins. Among the five top hit potential binding proteins, Dynamin-1-like protein (Drp1) levels were robustly elevated in GD3S-KO brains by Western blot analysis (Fig. 5D, E), which prompted us to examine more closely the significance of the interaction between GD3 and Drp1.

The GD3–Drp1 interaction was further verified by co-immunoprecipitation; mAb R24-immunoprecipitated Drp1 was detected in the WT brain lysate, but not in the GD3S-KO lysate (Fig. 5F). As Drp1 functions as a mitochondrial fission protein (Westermann 2010), we also imaged NSCs that were transfected with mito-dsRed and immunostained with Drp1 and GD3 antibodies. The 3D-reconstructed images demonstrated that Drp1 and GD3 were co-localized as puncta on mitochondria (Fig. 5G). A GSL-coated bead assay was also used to determine whether co-immunoprecipitation and co-localization of Drp1 and GD3 represent a direct physical interaction. We purified recombinant Drp1 protein from HEK293 cells transfected with His-Drp1 and incubated it with GSL-coated beads; Western blot analysis with anti-Drp1 antibody showed binding of His-Drp1 with GD3-coated polystyrene beads, but not with GM1-coated beads, demonstrating the specificity of the lipid-protein interaction (Fig. 5H). These experiments strongly suggest that Drp1 is a novel endogenous GD3-binding partner.

GD3 interacts with Drp1 to regulate mitochondrial morphology

The identification of Drp1 protein as a GD3 interactor was particularly interesting. Drp1 is a GTPase that regulates mitochondrial fission and plays important roles in the regulation of mitochondrial dynamics (Westermann 2010). Previous studies reported that enhancement of mitochondrial fission was sufficient to induce major alterations in dendritogenesis and synaptogenesis of neurons *in vitro* and disruption of mitochondrial dynamics in murine adult NSC-impaired hippocampus-dependent learning and memory (Arrazola et al. 2019;

Steib et al. 2014; Beckervordersandforth et al. 2017; Son & Han 2018). To investigate whether GD3 affects mitochondrial dynamics, we examined mitochondrial morphology in the nascent granule neurons. Retrovirus encoding for mitochondria-targeted dsRed (CAG-IRES-mito-dsRed) was co-injected with CAG-GFP into the DGs of GD3S-KO and control mice. Animals were sacrificed at different time intervals after retroviral injection (dpi) (Fig. 6A). At all the stages, mitochondria were of tubular morphology that had an average aspect ratio (major axis/minor axis) of more than two in WT neurons (Fig. 6B, C). In contrast, neurons with GD3S-KO had shorter mitochondria with an average aspect ratio around 1.6 (Fig. 6B, C), suggesting that mitochondria were fragmented. The neurite mitochondrial index (total mitochondrial length/neurite length), an index for mitochondrial density, was also significantly reduced in GD3S-KO neurons (Fig. 6D, E). These findings suggest that the loss of GD3 resulted in mitochondrial fragmentation in newborn DG neurons in adult brain.

To further validate the increased Drp1 expression in GD3S-KO brain (Fig. 6D, E), we isolated the mitochondrial fraction from DG. Western blot analysis demonstrated that Drp1 levels were slightly increased in GD3S-KO and the activated-Drp1 (phosphorylation of Drp1 at serine 616) was higher in GD3S-KO mitochondria (Fig. 7A, B). In contrast, we did not observe any significant changes for the fusion proteins Mfn2 (Fig. 7A, B). To confirm this finding, we imaged mitochondrial Drp1 in these nascent neurons. As shown in Fig. 7C, the density and average size of the mitochondrial Drp1 puncta were significantly increased in GD3S-KO neurons. To understand how GD3 regulates the Drp1 protein level, we measured the half-life of Drp1 in control and GD3S-KO neurons and found that the half-life of Drp1 in control cells was about 15 hours (Fig. 7D, E). However, it was dramatically increased in GD3S-KO neurons, with no detectable reduction within 20 hours of experiments. These findings suggest that GD3 may participate in regulating the clearance of mitochondrial Drp1 complexes.

Discussion

Dendrite development of nascent GCs in the DG of adult hippocampus is critical for their incorporation into existing hippocampal circuits, but the cellular mechanisms regulating dendrite development remains largely unclear. In this study, we found that GD3, which is expressed in newborn GCs in adult brain, plays an important role in regulating dendrite morphogenesis. Thus, GD3 is important for the maturation of nascent neurons in the adult mouse hippocampus by serving as a pivotal link between mitochondrial dynamics and maturation of the developing neurons.

GD3 in adult hippocampal neurogenesis and hippocampus-dependent memory function

In accordance with previous studies, we observed robust GD3 expression in the DG GC layer and in differentiating adult NSCs (Fig. 2). This expression pattern suggests that GD3 may regulate adult hippocampal neurogenesis in at least two different aspects: First, GD3 promotes NSC proliferation, thus, increasing the number of newborn neurons. This is supported by our previous observations that the reduced number of DCX+ immature neurons in GD3S-KO mice (Wang et al. 2014) compared well with the increased number of proliferative NSCs when GD3 was introduced *in vitro* and *in vivo* (Wang & Yu, 2013).

Second, GD3 enhances nascent neuronal maturation by increasing dendritic outgrowth and branching (Fig. 3). Meanwhile, analysis of 3D renderings of dendritic volumes demonstrated that GD3S-KO neurons exhibited reduced density of dendritic spines (Fig. 3). Dendritic spine development contributes to the initiation of the local dendritic spikes (Spruston 2008), suggesting that the morphological defects associated with deletion of GD3S may disturb synaptic inputs to the local circuit.

Hippocampal nascent neurons have been implicated in the acquisition and recall of hippocampus-dependent memories (Moreno-Jimenez et al. 2019; Gage 2019) and, therefore, adult hippocampal neurogenesis is an essential process for cognitive function (Zhao et al. 2006; Bond et al. 2015; Kang et al. 2016). In this investigation, we demonstrated that both control and GD3S-KO mice acquired a basic procedural task, specifically, locating a visible escape box in the initial phase of the Barnes maze. However, only control animals learned, and subsequently recalled, the portion of the task that required generating a spatial map to locate the platform. GD3S-KO mice never acquired this behavior, suggesting a selective hippocampal-dependent learning deficit (Fig. 4). The deficits we found in morphology and integration of adult-born neurons in the absence of GD3 may therefore contribute to the learning deficits exhibited by these mice. The reduced arborization of GD3S-KO neurons conceivably created a shortage of the receptive field for inputs, which could disrupt the specificity of incoming excitatory stimuli to GCs. Reduced dendritic spine density could further alter the organization of excitatory inputs and reduce the number of contacts received by each neuron (Spruston 2008; Winkle et al. 2016). As GCs are selectively recruited by incoming stimuli, which facilitate learning and memory, sensory integration, and pattern separation (Abrous & Wojtowicz 2015), this could produce significant defects in any of these cognitive processes. Previously, deletion of GD3 synthase was reported only to exert beneficial effects on the cognition of APP/PSEN1 transgenic mice and to protect against MPTP-induced neurodegeneration. (Bernardo et al. 2009; Akkhawattanangkul et al. 2017). This beneficial effect of ablation of GD3 synthase, however, was not observed when comparison was made with the wild-type control. Therefore, when considering using GD3S as a therapeutic target, it is important to consider its side effects.

Regulation of mitochondrial dynamics by GD3-Drp1 interaction in nascent neurons of the adult hippocampus

GSL-enriched microdomains, also known as lipid rafts, are normally detected at the cell plasma membranes, where they exert an essential function facilitating molecular interactions and signal transduction (Schnaar 2016). Under pre-apoptotic stimulation, the presence of raft-like microdomains at the mitochondrial level has also been demonstrated (Garofalo et al. 2005). It has been hypothesized that they could contribute to mitochondrial remodeling, e.g., fission processes and changes of membrane curvature associated with apoptosis (Ciarlo et al. 2010). GD3 is involved in *Fas*-mediated apoptosis in hematopoietic cells, causing the loss of mitochondrial potential and the release of apoptotic factors (De Maria et al. 1997; Tomassini & Testi 2002). Thus, GD3 is not only localized in the plasma membranes, but is also present in the cytosol and other intracellular structures, including the endoplasmic reticulum- and mitochondrion-associated, and nuclear membranes, where they play important functional roles (Sorice et al. 2010; Yu et al, 2012; Sorice et al. 2009). In the present context, we

found for the first time the binding of the mitochondrial fission protein Drp1 with GD3 using a proteomic approach. This interaction was corroborated by the co-localization of Drp1 puncta and GD3 on mitochondria and endogenously co-immunoprecipitated Drp1 by the GD3-specific antibody (Fig. 5). Importantly, these results came from analyses performed in fresh brain tissues. This is consistent with a recent brain mitochondrial lipidomic study showing the detection of gangliosides in mouse brain mitochondria (Kiebish et al. 2008).

The importance of the ganglioside-protein molecular interaction has already been widely recognized. In particular, it has been hypothesized that ganglioside-protein complexes may act as regulators of membrane organization and be involved in the pathogenesis of human diseases (Schnaar 2016; Yu et al. 2012; Sandhoff et al. 2018). Recently, we have provided direct evidence that the GD3-containing microdomains act as a platform to initiate and facilitate EGF trafficking and degradation in cultured NSCs (Wang & Yu 2013). Here, we report that Drp1 is upregulated in GD3S-KO brain. Because Drp1 plays a key role in mitochondrial fission, we investigated if loss of GD3 affected the translocation of Drp1 to mitochondria. In isolated mitochondrial fractions from GD3S-KO DG, we observed an increased level of Drp1. In addition, we found a significant increase in mitochondrial Drp1 puncta in GD3S-KO nascent neurons (Fig. 7). Mechanistically, we can only speculate that GD3 affects Drp1 protein turnover based on the observation that loss of GD3 altered Drp1 half-life after treatment with cycloheximide (Fig. 7). Interestingly, Drp1 can also be modified by O-GlcNAcylation (Gawlowski et al. 2012). In cardiomyocytes, excessive O-GlcNAcylation translocates Drp1 to mitochondria and augments mitochondrial fragmentation and impairs mitochondrial function (Gawlowski et al. 2012). As the interaction between gangliosides and proteins are dependent on the glycan chains, it would be of interest to further investigate how Drp1 O-GlcNAcylation could influence GD3-Drp1 binding.

In vitro findings indicated that mitochondrial fusion and fission alter bioenergetics, which in turn influence neuronal morphogenesis (Dickey & Strack 2011). In addition, mitochondrial morphology is related to mitochondrial biogenesis, and mitochondrial fission is crucial for efficient distribution of new mitochondria to the growing axons and dendritic trees in cultured neurons (Li et al. 2004). Mitochondrial fission relies on the activity of GTPase associated with Drp1. Drp1 forms helical oligomers that wrap around the mitochondrial outer membrane and scissions it (Westermann 2010). The functional properties of Drp1 are modulated by a number of posttranslational modifications, including phosphorylation (Chang & Blackstone 2007; Cereghetti et al. 2008). As shown in Fig. 7, we have seen increased phosphorylation of Drp1 at Ser-616 in GD3S-KO mitochondria. As phosphorylation of Ser-616 promotes mitochondrial fission (Chang & Blackstone 2007), mitochondrial fragmentation was shown in GD3S-KO nascent neurons (Fig. 6). The fewer number of mitochondria in GD3S-KO dendrites is coupled with less dendritic arborization and reduced spine formation (Fig. 7C). Taken together, these results support the notion that mitochondrial fission constitutes a limiting factor on dendritogenesis and spinogenesis in adult neurogenesis.

In conclusion, the present study provides novel information on the role of ganglioside GD3 in the maturation of nascent hippocampal granule neurons by regulating mitochondrial

dynamics through binding with Drp1. We propose a working model (Fig. 7F) in which GD3 mediates the removal of Drp1 from mitochondria and transports it to lysosomes for degradation, a process that is likely required for efficient mitochondrial fission, thereby regulating mitochondrial function and dendritogenesis / spinogenesis, which contributes to the hippocampus-dependent memory function. Since GSLs are known to strongly influence the biophysical properties of biomembranes as well as their curvature (Maggio et al. 1990), we speculate that ganglioside GD3 may play a pivotal role in morphogenic remodeling of mitochondria during the development of newly generated neurons in adult brain. A better understanding of the role of ganglioside GD3 in mitochondrial function may thus provide useful insights in basic as well as in translational medicine.

Acknowledgments

This work was supported by an NIH grant (R01 NS100839) and a Sheffield Memorial Award from CSRA Parkinson Support Group to RKY. We thank Dr. Yong Li and the Small Animal Behavioral Core, AU, for discussion and help with the behavior analysis.

Abbreviations:

DG	Dentate gyrus
KO	Knockout
GSL	Glycosphingolipid
NSC	Neural stem cell
NPC	Neural progenitor cell
GCL	Granule cell layer
SGZ	Subgranular zone

References

Abrous DN and Wojtowicz JM (2015) Interaction between Neurogenesis and Hippocampal Memory System: New Vistas. Cold Spring Harb Perspect Biol 7.

Akkhawattanangkul Y, Maiti P, Xue Y, Aryal D, Wetsel WC, Hamilton D, Fowler SC and McDonald MP (2017) Targeted deletion of GD3 synthase protects against MPTP-induced neurodegeneration. Genes Brain Behav 16, 522–536. [PubMed: 28239983]

Arrazola MS, Andraini T, Szelechowski M, Mouledous L, Arnaune-Pelloquin L, Davezac N, Belenguer P, Rampon C and Miquel MC (2019) Mitochondria in Developmental and Adult Neurogenesis. Neurotox Res 36, 257–267. [PubMed: 30215161]

Beckervordersandforth R, Ebert B, Schaffner Iet al. (2017) Role of Mitochondrial Metabolism in the Control of Early Lineage Progression and Aging Phenotypes in Adult Hippocampal Neurogenesis. Neuron 93, 560–573 e566. [PubMed: 28111078]

Bernardo A, Harrison FE, McCord Met al. (2009) Elimination of GD3 synthase improves memory and reduces amyloid-beta plaque load in transgenic mice. Neurobiol Aging 30, 1777–1791. [PubMed: 18258340]

Bird AD and Cuntz H (2019) Dissecting Sholl Analysis into Its Functional Components. Cell Rep 27, 3081–3096 e3085. [PubMed: 31167149]

Bond AM, Ming GL and Song H (2015) Adult Mammalian Neural Stem Cells and Neurogenesis: Five Decades Later. Cell Stem Cell 17, 385–395. [PubMed: 26431181]

Cereghetti GM, Stangherlin A, Martins de Brito O, Chang CR, Blackstone C, Bernardi P and Scorrano L (2008) Dephosphorylation by calcineurin regulates translocation of Drp1 to mitochondria. Proc Natl Acad Sci U S A 105, 15803–15808. [PubMed: 18838687]

Chandel NS (2014) Mitochondria as signaling organelles. BMC Biol 12, 34. [PubMed: 24884669]

Chang CR and Blackstone C (2007) Cyclic AMP-dependent protein kinase phosphorylation of Drp1 regulates its GTPase activity and mitochondrial morphology. J Biol Chem 282, 21583–21587. [PubMed: 17553808]

Ciarlo L, Manganelli V, Garofalo T, Matarrese P, Tinari A, Misasi R, Malorni W and Sorice M (2010) Association of fission proteins with mitochondrial raft-like domains. Cell Death Differ 17, 1047–1058. [PubMed: 20075943]

De Maria R, Lenti L, Malisan F, d'Agostino F, Tomassini B, Zeuner A, Rippo MR and Testi R (1997) Requirement for GD3 ganglioside in CD95- and ceramide-induced apoptosis. Science 277, 1652–1655. [PubMed: 9287216]

Dickey AS and Strack S (2011) PKA/AKAP1 and PP2A/Bbeta2 regulate neuronal morphogenesis via Drp1 phosphorylation and mitochondrial bioenergetics. J Neurosci 31, 15716–15726. [PubMed: 22049414]

Ennaceur A and Delacour J (1988) A new one-trial test for neurobiological studies of memory in rats. 1: Behavioral data. Behav Brain Res 31, 47–59. [PubMed: 3228475]

Gage FH (2019) Adult neurogenesis in mammals. Science 364, 827–828. [PubMed: 31147506]

Garcia-Ruiz C, Colell A, Morales A, Calvo M, Enrich C and Fernandez-Checa JC (2002) Trafficking of ganglioside GD3 to mitochondria by tumor necrosis factor-alpha. J Biol Chem 277, 36443–36448. [PubMed: 12118012]

Garofalo T, Giammarioli AM, Misasi R, Tinari A, Manganelli V, Gambardella L, Pavan A, Malorni W and Sorice M (2005) Lipid microdomains contribute to apoptosis-associated modifications of mitochondria in T cells. Cell Death Differ 12, 1378–1389. [PubMed: 15947792]

Gawlowski T, Suarez J, Scott Bet al. (2012) Modulation of dynamin-related protein 1 (DRP1) function by increased O-linked-beta-N-acetylglucosamine modification (O-GlcNAc) in cardiac myocytes. J Biol Chem 287, 30024–30034. [PubMed: 22745122]

Hagihara H, Toyama K, Yamasaki N and Miyakawa T (2009) Dissection of hippocampal dentate gyrus from adult mouse. J Vis Exp.

Harrison FE, Hosseini AH and McDonald MP (2009) Endogenous anxiety and stress responses in water maze and Barnes maze spatial memory tasks. Behav Brain Res 198, 247–251. [PubMed: 18996418]

Kang E, Wen Z, Song H, Christian KM and Ming GL (2016) Adult Neurogenesis and Psychiatric Disorders. Cold Spring Harb Perspect Biol 8.

Kiebish MA, Han X, Cheng H, Lunceford A, Clarke CF, Moon H, Chuang JH and Seyfried TN (2008) Lipidomic analysis and electron transport chain activities in C57BL/6J mouse brain mitochondria. J Neurochem 106, 299–312. [PubMed: 18373617]

Li Z, Okamoto K, Hayashi Y and Sheng M (2004) The importance of dendritic mitochondria in the morphogenesis and plasticity of spines and synapses. Cell 119, 873–887. [PubMed: 15607982]

Lu Y, Sareddy GR, Wang Jet al. (2019) Neuron-Derived Estrogen Regulates Synaptic Plasticity and Memory. J Neurosci 39, 2792–2809. [PubMed: 30728170]

Maggio B, Ariga T and Yu RK (1990) Ganglioside GD3 lactones: polar head group mediated control of the intermolecular organization. Biochemistry 29, 8729–8734. [PubMed: 2271553]

Moreno-Jimenez EP, Flor-Garcia M, Terreros-Roncal J, Rabano A, Cafini F, Pallas-Bazarra N, Avila J and Llorens-Martin M (2019) Adult hippocampal neurogenesis is abundant in neurologically healthy subjects and drops sharply in patients with Alzheimer's disease. Nat Med 25, 554–560. [PubMed: 30911133]

Pukel CS, Lloyd KO, Travassos LR, Dippold WG, Oettgen HF and Old LJ (1982) GD3, a prominent ganglioside of human melanoma. Detection and characterisation by mouse monoclonal antibody. J Exp Med 155, 1133–1147. [PubMed: 7061953]

Rippo MR, Malisan F, Ravagnan Let al. (2000) GD3 ganglioside directly targets mitochondria in a bcl-2-controlled fashion. FASEB J 14, 2047–2054. [PubMed: 11023989]

Rosner H, al-Aqtum M and Rahmann H (1992) Gangliosides and neuronal differentiation. Neurochem Int 20, 339–351. [PubMed: 1304329]

Sandhoff R, Schulze H and Sandhoff K (2018) Ganglioside Metabolism in Health and Disease. Prog Mol Biol Transl Sci 156, 1–62. [PubMed: 29747811]

Savas JN, Ribeiro LF, Wierda KDet al. (2015) The Sorting Receptor SorCS1 Regulates Trafficking of Neurexin and AMPA Receptors. Neuron 87, 764–780. [PubMed: 26291160]

Schaffner I, Minakaki G, Khan MAet al. (2018) FoxO Function Is Essential for Maintenance of Autophagic Flux and Neuronal Morphogenesis in Adult Neurogenesis. Neuron 99, 1188–1203 e1186. [PubMed: 30197237]

Schnaar RL (2016) Gangliosides of the Vertebrate Nervous System. J Mol Biol 428, 3325–3336. [PubMed: 27261254]

Schnaar RL, Gerardy-Schahn R and Hildebrandt H (2014) Sialic acids in the brain: gangliosides and polysialic acid in nervous system development, stability, disease, and regeneration. Physiol Rev 94, 461–518. [PubMed: 24692354]

Son G and Han J (2018) Roles of mitochondria in neuronal development. BMB Rep 51, 549–556. [PubMed: 30269744]

Sorice M, Matarrese P, Manganelli V, Tinari A, Giammarioli AM, Mattei V, Misasi R, Garofalo T and Malorni W (2010) Role of GD3-CLIPR-59 association in lymphoblastoid T cell apoptosis triggered by CD95/Fas. PLoS One 5, e8567. [PubMed: 20052288]

Sorice M, Matarrese P, Tinari Aet al. (2009) Raft component GD3 associates with tubulin following CD95/Fas ligation. FASEB J 23, 3298–3308. [PubMed: 19509307]

Spruston N (2008) Pyramidal neurons: dendritic structure and synaptic integration. Nat Rev Neurosci 9, 206–221. [PubMed: 18270515]

Steib K, Schaffner I, Jagasia R, Ebert B and Lie DC (2014) Mitochondria modify exercise-induced development of stem cell-derived neurons in the adult brain. J Neurosci 34, 6624–6633. [PubMed: 24806687]

Sun D, Sun XD, Zhao Let al. (2018) Neogenin, a regulator of adult hippocampal neurogenesis, prevents depressive-like behavior. Cell Death Dis 9, 8. [PubMed: 29311593]

Tang FL, Liu W, Hu JX, Erion JR, Ye J, Mei L and Xiong WC (2015) VPS35 Deficiency or Mutation Causes Dopaminergic Neuronal Loss by Impairing Mitochondrial Fusion and Function. Cell Rep 12, 1631–1643. [PubMed: 26321632]

Tang FL, Zhao L, Zhao Y, Sun D, Zhu XJ, Mei L and Xiong WC (2020) Coupling of terminal differentiation deficit with neurodegenerative pathology in Vps35-deficient pyramidal neurons. Cell Death Differ.

Tomassini B and Testi R (2002) Mitochondria as sensors of sphingolipids. Biochimie 84, 123–129. [PubMed: 12022943]

Wang J, Cheng A, Wakade C and Yu RK (2014) Ganglioside GD3 is required for neurogenesis and long-term maintenance of neural stem cells in the postnatal mouse brain. J Neurosci 34, 13790–13800. [PubMed: 25297105]

Wang J and Yu RK (2013) Interaction of ganglioside GD3 with an EGF receptor sustains the self-renewal ability of mouse neural stem cells in vitro. Proc Natl Acad Sci U S A 110, 19137–19142. [PubMed: 24198336]

Wang W, Wang X, Fujioka H, Hoppel C, Whone AL, Caldwell MA, Cullen PJ, Liu J and Zhu X (2016) Parkinson’s disease-associated mutant VPS35 causes mitochondrial dysfunction by recycling DLP1 complexes. Nat Med 22, 54–63. [PubMed: 26618722]

Westermann B (2010) Mitochondrial fusion and fission in cell life and death. Nat Rev Mol Cell Biol 11, 872–884. [PubMed: 21102612]

Winkle CC, Olsen RH, Kim H, Moy SS, Song J and Gupton SL (2016) Trim9 Deletion Alters the Morphogenesis of Developing and Adult-Born Hippocampal Neurons and Impairs Spatial Learning and Memory. J Neurosci 36, 4940–4958. [PubMed: 27147649]

Yanagisawa M, Taga T, Nakamura K, Ariga T and Yu RK (2005) Characterization of glycoconjugate antigens in mouse embryonic neural precursor cells. J Neurochem 95, 1311–1320. [PubMed: 16219035]

Yoon SJ, Nakayama K, Hikita T, Handa K and Hakomori SI (2006) Epidermal growth factor receptor tyrosine kinase is modulated by GM3 interaction with N-linked GlcNAc termini of the receptor. Proc Natl Acad Sci U S A 103, 18987–18991. [PubMed: 17142315]

Yu RK and Ando S (1980) Structures of some new complex gangliosides of fish brain. Adv Exp Med Biol 125, 33–45. [PubMed: 7361620]

Yu RK, Tsai YT and Ariga T (2012) Functional roles of gangliosides in neurodevelopment: an overview of recent advances. Neurochem Res 37, 1230–1244. [PubMed: 22410735]

Yu RK, Tsai YT, Ariga T and Yanagisawa M (2011) Structures, biosynthesis, and functions of gangliosides--an overview. J Oleo Sci 60, 537–544. [PubMed: 21937853]

Zhao C, Teng EM, Summers RG Jr., Ming GL and Gage FH (2006) Distinct morphological stages of dentate granule neuron maturation in the adult mouse hippocampus. J Neurosci 26, 3–11. [PubMed: 16399667]

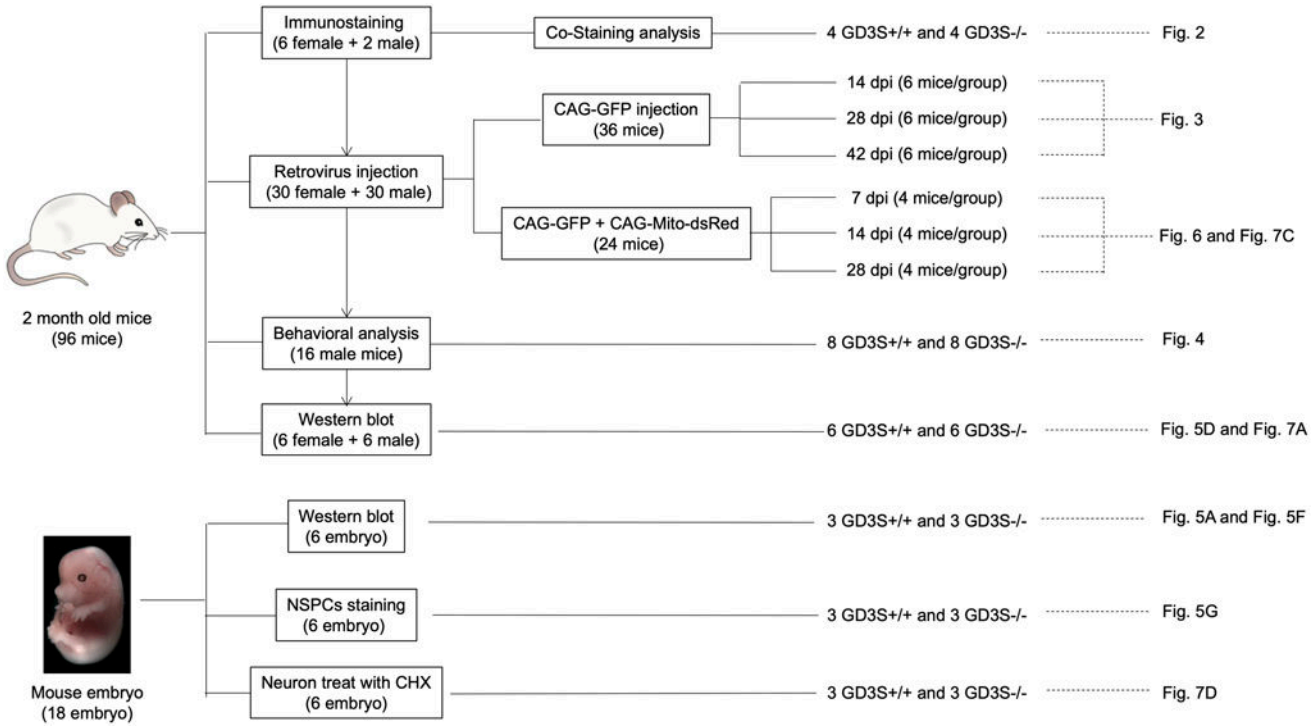

Figure 1.
Scheme of animals, experiments and corresponding figures.

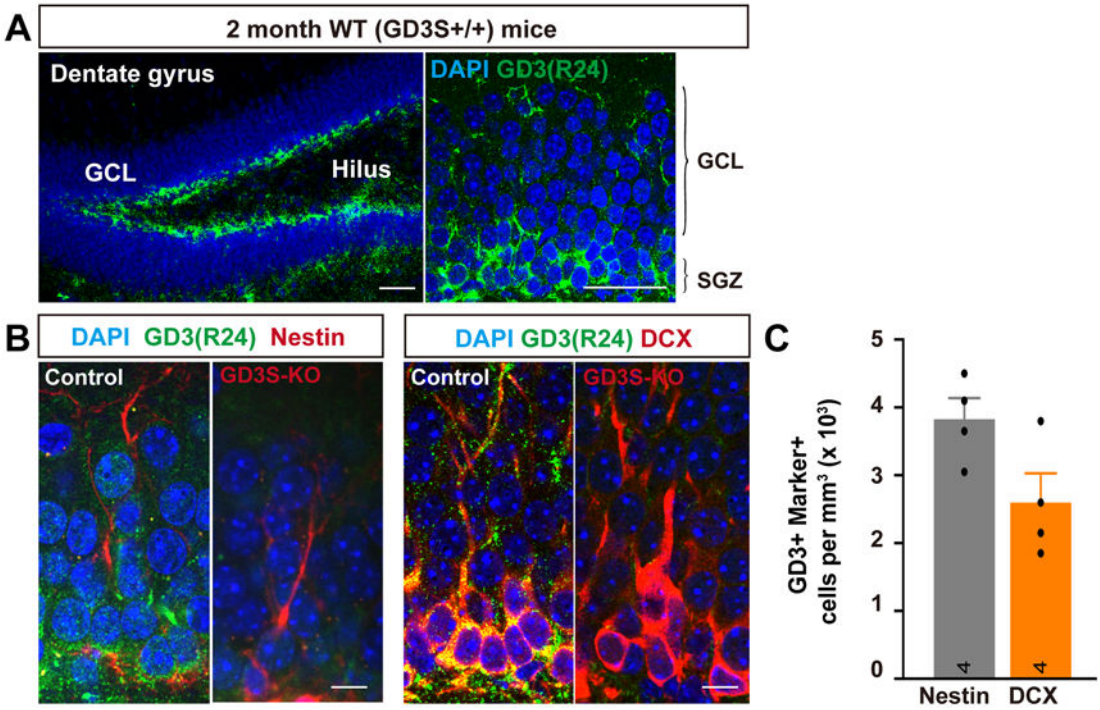

Figure 2. GD3 is expressed in NSCs and immature neurons of the adult mouse hippocampus.

(A) Representative immunodetection of GD3 in the dentate gyrus of 2-month-old mice. Scale bar: 50 μm. GCL: granule cell layer, SGZ: subgranular zone. **(B)** Co-expression of GD3 with Nestin and DCX in cells of the SGZ in the dentate gyrus of 2-month-old mice. Scale bar: 10 μm. **(C)** Quantification of the number of GD3+ cells; Nestin+ and GD3+ cells; DCX+ cells in DG. (n = 4 mice / group).

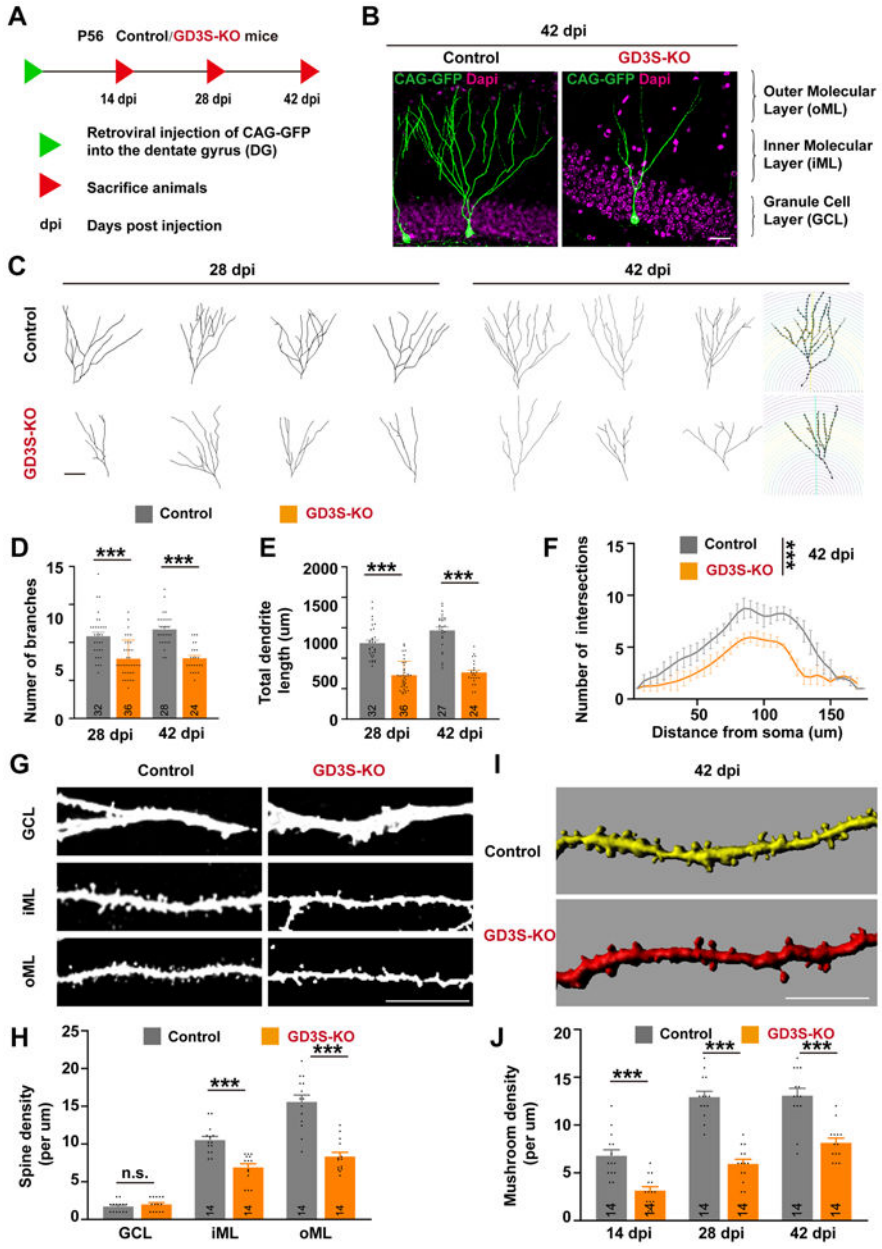

Figure 3. Effects of GD3 deletion in adult-born granule cells (GCs) on dendritic development.

(A) Schematic diagram showing the experimental procedure for labeling nascent GCs in adult mice through retrovirus-mediated gene transfection. Mice were perfused at different time points as indicated. dpi, days post infection. **(B)** Retrovirus infected nascent neurons in WT and GD3S-KO mice at 42 dpi. Scale bars, 10 μm. **(C)** Representative reconstructions of WT and GD3S-KO neurons. Scale bars, 10 μm. **(D-E)** Quantification of the number of branches (D) and total dendritic length (E) at 28 and 42 dpi. n = 32/28 (28/42 dpi) Control and n = 36/24 (28/42 dpi) GD3S-KO neurons from 6 mice/group. **(F)** Sholl analyses of dendritic intersections from neuronal soma. (n=6 neurons from 6 mice/group; two-way ANOVA with a Tukey's multiple comparisons test). **(G)** Representative images showing dendritic segments in different layers of the DG. Note the decreased spine density

and abnormal spine formation in the GCL of GD3S-KO mice. Scale bars, 10 μm. **(H)** Quantification of the number of spines in WT and GD3S-KO neurons at 42 dpi. n = 14 neurons from 6 mice/group. **(I)** Representative 3D-reconstructed dendritic spines. **(J)** Quantification of mushroom spine density at different stages. n = 14 neurons from 6 mice/group. ***, $p < 0.001$; n.s., not significant.

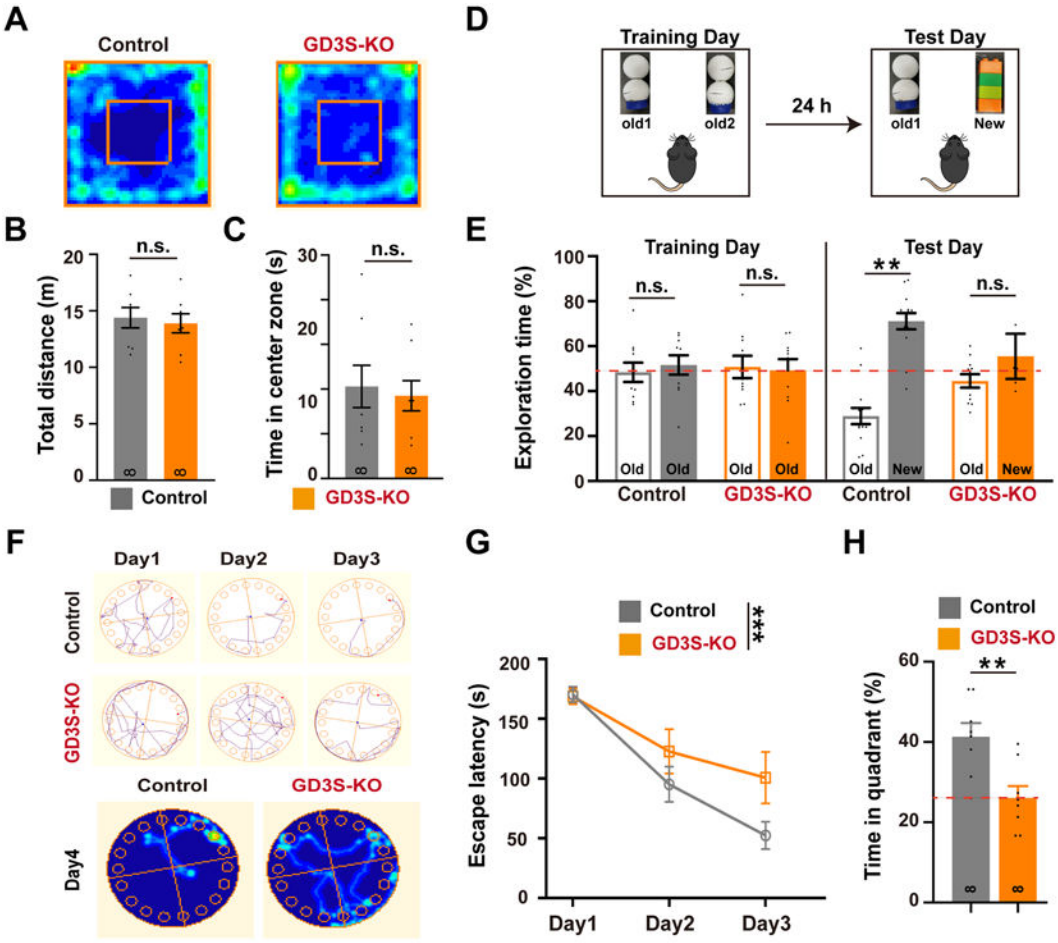

Figure 4. Ablation of GD3 impairs hippocampus-dependent memory.

(A) Representative heat maps illustrating the time spent in different locations of the arena for open field test. **(B)** Travel distance and **(C)** time in center zone showed no alterations in GD3S-KO mice compared with control. **(D)** Schematic diagram showing the experimental procedure of NOR test. **(E)** Percentage of exploration time between old and new object locations in the NOR test for WT and GD3S-KO. **(F)** Upper: Representative tracking plots of WT and GD3S-KO mice on Barnes maze training trials. Lower: Representative heat maps illustrating the time spent in different locations of the arena for Barnes maze tests during the memory phase (escape box removed) in control and GD3S-KO mice. **(G)** Time spent to find the escape box during the Barnes maze training sessions in both control and GD3S-KO mice. **(H)** Bar graphs showing the time spent on exploring the correct quadrant in the memory phase of Barnes maze tests. For all behavior test, n = 8 / group. $^{**}p < 0.01$; n.s., not significant.

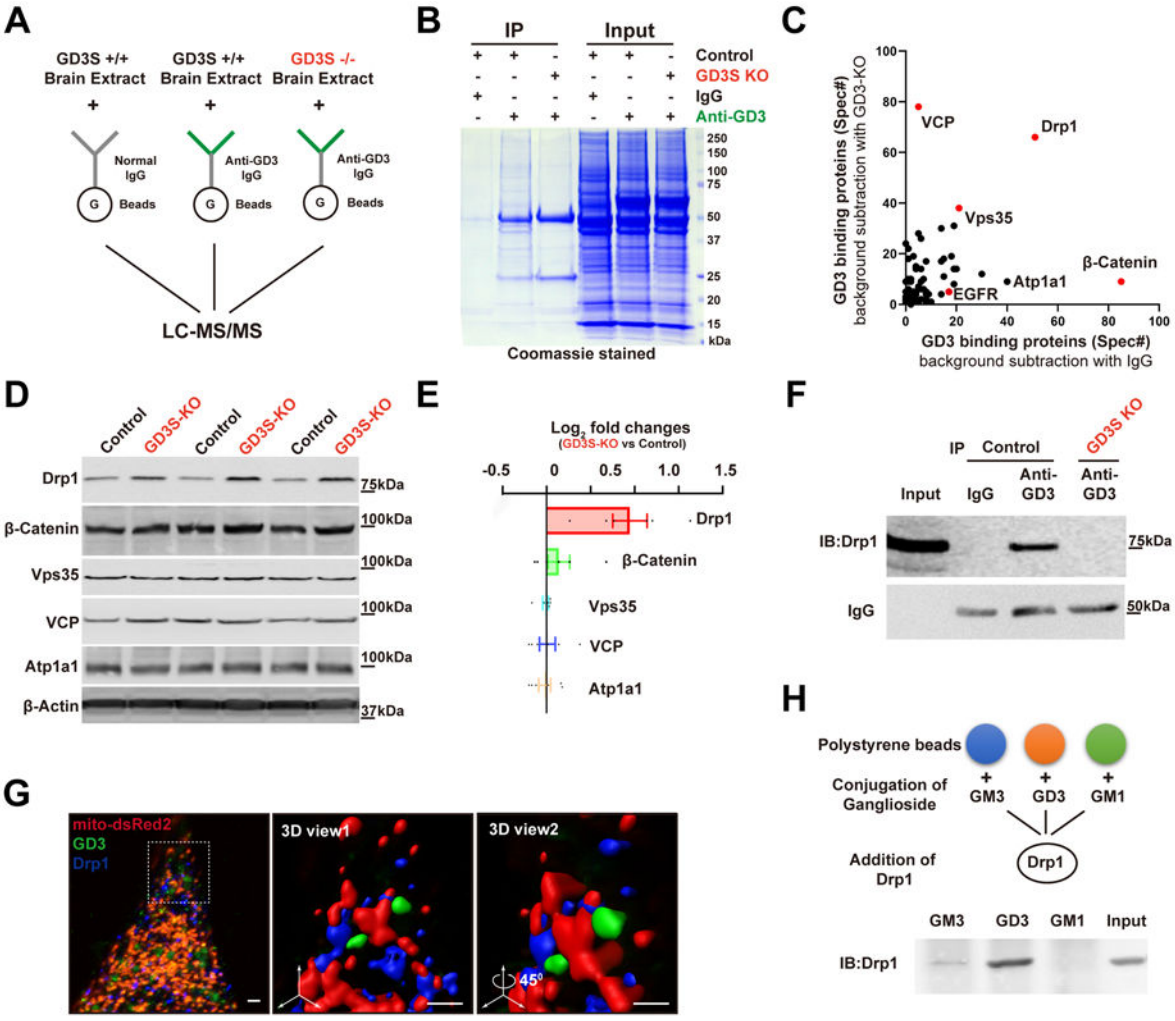

Figure 5. Identification of Drp1 as a GD3-binding protein.

(A) Proteomic workflow for the identification of GD3-interacting proteins. **(B)** Representative Coomassie-stained SDS gel of proteins bound to bead-coupled anti-GD3 antibody incubated with brain extracts, with indicated negative control. **(C)** Frequency of detection of all peptides (total spectra count) for proteins identified. **(D)** Lysates (30 μg protein) of DG were immunoblotted with the indicated antibodies. **(E)** Quantification of data from (D) (normalized by control). n = 6 mice / group. **(F)** Representative Western blot analyses for the presence of immunoprecipitates. **(G)** Representative 3D images showing the co-localization of endogenous GD3 and Drp1 on mitochondria in NSCs with mito-DsRed2 and immunostained with anti-Drp1 and mAb R24. Boxed area in the left image was enlarged and viewed at different angles. Scale bars, 1 μm. **(H)** Interaction of GSL-coated polystyrene beads with Drp1.

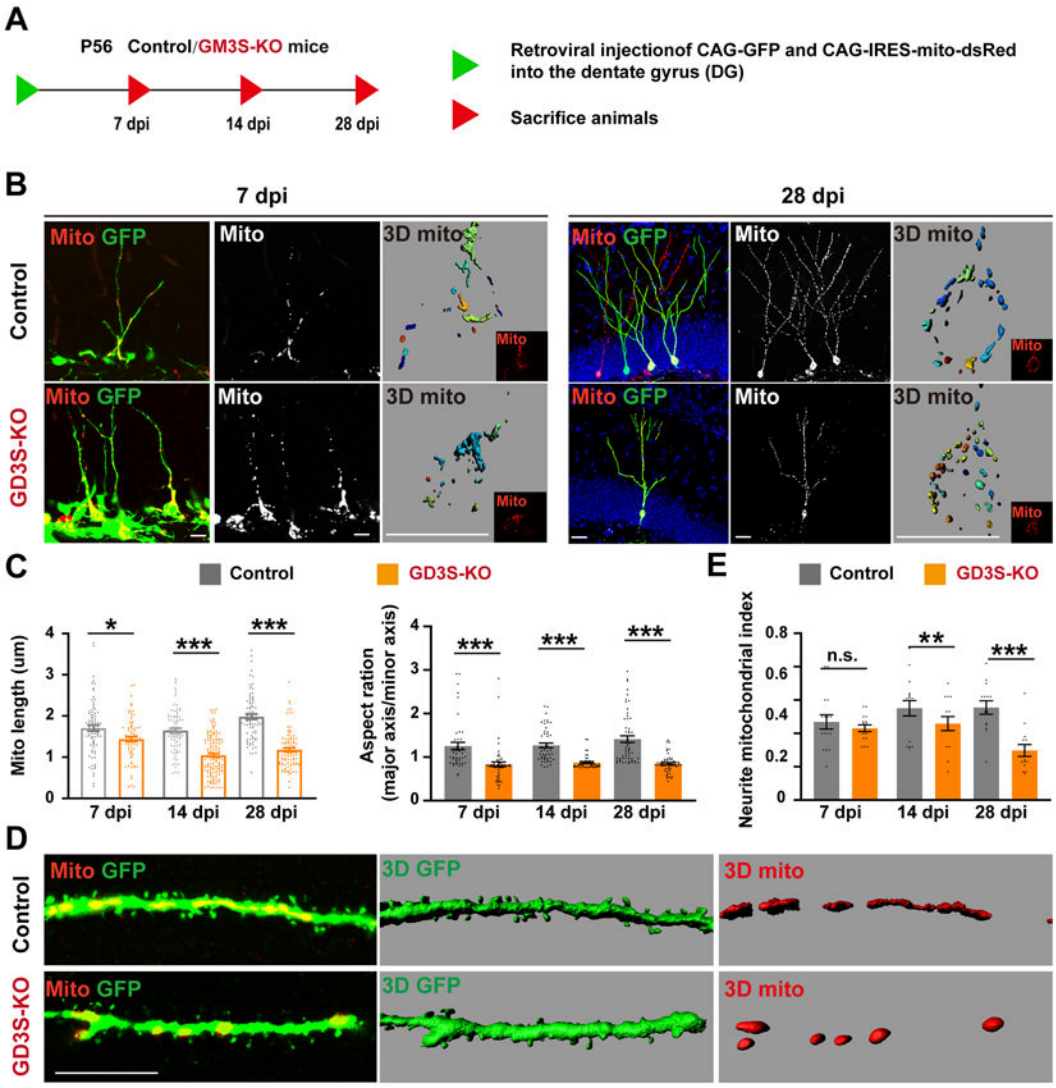

Figure 6. GD3 regulates mitochondrial dynamics *in vivo*.

(A) Experimental scheme of visualization of mitochondria and cell morphology in adult-born neurons. **(B)** Representative confocal and 3D pictures (last one) of mitochondria in nascent neurons in adult brain. **(C)** Quantification of mitochondrial length, aspect ratio and percentage of neurons with fragmented mitochondria in adult newborn neurons. n = 100 mitochondria from 4 mice / groups. **(D)** A segment of dendrites was enlarged. **(E)** Quantification of neurite-mitochondrial index (total mitochondrial length/neurite length), an index for mitochondrial density. n = 16 neurites from 4 mice / group.

Panel C on the right: y axis should be aspect ratio, not ration.

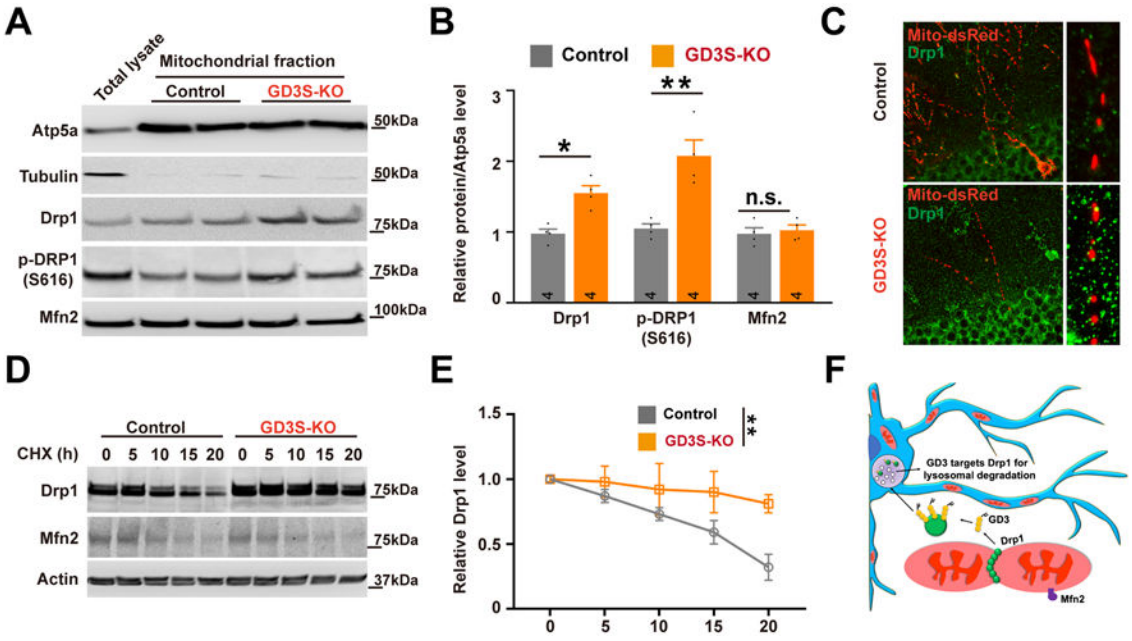

Figure 7. GD3 regulates mitochondrial Drp1 complex turnover.

(A-B) Representative Western blot (A) and quantification (B) of Drp1 in mitochondrial fractions from DG of control and GD3S-KO mice. n = 6 mice / group. **(C)** Representative confocal images of Drp1 (green) and mitochondria (red), demonstrating mitochondrial Drp1 puncta. **(D-E)** After neurons were treated with cycloheximide (CHX; 50 μg/mL) for the indicated time, expression of Drp1 and Mfn2 was analyzed by Western blotting (D); the intensity of Drp1 expression for each time point was quantified by densitometry, with tubulin as a normalizer (E). n = 6 mice / group. **(F)** Schematic representation of the role of GD3 in the regulation of mitochondrial dynamics by mediating the turnover of mitochondrial Drp1. *$p < 0.05$; **$p < 0.01$.